RED CELL AGGREGATION BY MACROMOLECULES: ROLES OF SURFACE ADSORPTION AND ELECTROSTATIC REPULSION

Shu Chien and Kung-ming Jan

Laboratory of Hemorheology, Department of Physiology, College of Physicians and Surgeons, Columbia University, New York, New York 10032

Aggregation of normal and neuraminidase-treated human red blood cells (RBC) by dextrans of various molecular sizes and concentrations was quantified by microscopic counting and light reflectometry. The influences of variations in the ionic strength and the cationic valency of the dextran solution on RBC aggregation were also investigated. The data on RBC aggregation were correlated with measurements of the zeta potential by cell electrophoresis and the intercellular distance in the rouleaux by electron microscopy. With the use of the classical equations and newly developed knowledge in colloid chemistry, the electrostatic repulsive force between adjacent cell surfaces (F_e) was calculated from the experimental data. The macromolecular bridging force causing RBC aggregation (F_b) has also been derived as a function of dextran concentration. Other forces that cause RBC disaggregation are the mechanical shearing force (F_s) and the RBC membrane bending force (F_m). The net force for RBC aggregation is equal to $F_b - F_e - F_m - F_s$. This model of aggregation involving force balance at the surface can explain known experimental results on factors influencing cell aggregation. It is proposed that such force balance between cell surfaces may be applicable in other cell or particulate systems and that it may be of fundamental importance in many physiological functions.

Cell to cell interaction is a fundamental phenomenon in biology and medicine. Cell aggregation and disaggregation are of considerable importance in development, growth, differentiation, and functioning of the multicellular organism under physiological conditions and they also play an important role in many pathological states, e.g., the growth and metastasis of tumor cells. Since the red blood cell (RBC) is probably the most easily obtainable and controllable among cells, it represents an excellent candidate for studying interactions between cell surfaces. Of course, each cell type presents different structural and functional features which prevent direct extrapolation from the results obtained on RBC to other cells. Nevertheless, an elucidation of the biophysical nature of the RBC interactions may yield some basic information which can be applied to other cell systems with appropriate modifications.

Red blood cells are monodispersed in isotonic salt solutions, and RBC aggregation requires the presence of macromolecules in the suspending medium. The classical studies of Fåhraeus (1) have demonstrated that the physicochemical properties and the concentration of the macromolecules play a significant role in affecting RBC aggregation, suggesting that RBC aggregation results from an interaction of the macromolecules with

Journal of Supramolecular Structure

the RBC. Since the RBC surface is negatively charged (2), RBC aggregation may involve a balance between the attractive force and the electrostatic repulsive force. There is, however, a lack of definitive information concerning the significance of the surface charge in RBC aggregation. This is attributable to technical limitation in quantifying red cell aggregation, the lack of control of the variables in the system, and deficiency in theoretical treatment of the influence of macromolecular adsorption on potential distribution near the cell surface. Several techniques for the quantification of RBC aggregation have been developed in our laboratory, and they have been applied to the study of the role of electrostatic repulsion in affecting RBC aggregation induced by various macromolecules, especially the neutral polymer dextrans. The variables in the system, including RBC surface charge, macromolecular size and concentration, ionic strength and valency, and mechanical shearing force, have been systematically varied and controlled. The experimental data have been analyzed with the aid of the theoretical treatment established in colloid chemistry (3), with modifications according to the recent model developed by Brooks (4). The results of these studies have provided quantitative information on the role of electrostatic repulsive force in affecting RBC aggregation. It has been established that RBC aggregation represents a balance of forces at the cell surfaces, and aggregation results when the macromolecular bridging force exceeds the electrostatic repulsive force and the mechanical shearing force. This communication combines some of the results recently reported from this laboratory (5–9) with additional data which have not yet been published.

METHODS

Normal and Neuraminidase-treated Red Cells

Fresh blood samples were collected from normal human subjects with heparin as an anticoagulant. After centrifugation and removal of the plasma and buffy coat, the RBC were washed 3 times with 150 mM NaCl solution or other solutions as indicated. The solutions were adjusted to a pH of 7.4 with tris buffer which contained 0.5 g% human serum albumin for the prevention of crenation (10).

For the enzymatic removal of RBC surface charge, neuraminidase prepared from Clostridium perfringens (Sigma Chemical Co., St. Louis, Mo.) was added to suspensions of 1% RBC in 150 mM NaCl solution which were then incubated at 37°C. After preliminary studies on the effect of neuraminidase concentration and incubation duration (see **RESULTS**), a concentration of 15 μg/ml and a duration of 60 minutes were adopted.

Suspending Medium

The macromolecules used to induce RBC aggregation were dextrans with various molecular weights (Pharmacia Labs., Uppsala, Sweden). The mean molecular weights of the dextrans used are listed in Table I. The dextrans were dissolved in 150 mM NaCl solution with a concentration range of 0–10 g% (grams of dextran per 100 ml of NaCl solution).

In order to study the influence of cation valency on RBC aggregation, dextrans were also dissolved in 150 mM salt solutions containing 0–10 mM of $MgCl_2$, $CaCl_2$, or $BaCl_2$ (balance NaCl). For studying the effect of ionic strength on RBC aggregation, dextran solutions were prepared in isoosmotic mixtures of 150 mM NaCl and 300 mM sucrose in

TABLE I. Molecular Weight of Dextrans

Dextran fractions	Weight-average molecular weight
Dx 20	20×10^3
Dx 40	42×10^3
Dx 80	74×10^3
Dx 150	141×10^3
Dx 500	450×10^3
Dx 2000	2000×10^3

various ratios. All dextran solutions contained 0.5 g% human serum albumin and the pH was adjusted to 7.4 with tris buffer.

Electrophoretic Measurements

The electrophoretic mobility of RBC suspended in various media at a cell concentration of 0.1% was measured in a cylindrical microelectrophoresis apparatus (Grant Instruments, Cambridge, England) at a temperature of 25°C. The velocity of migration of the RBC was measured microscopically at the stationary level (11), and the electrophoretic mobility (u, in μm sec^{-1}/volt cm^{-1}) was calculated as the ratio of the velocity to the applied voltage gradient. For each sample, 20 measurements were made in alternate directions. The zeta potential (ζ) was calculated with the use of the Helmholtz–Smoluchowski equation (3)

$$\zeta = 360\pi\eta u/D \tag{1}$$

where η is the viscosity (in centipoises) and D is the dielectric constant of the fluid medium. The viscosity of the electrophoretic media (dextrans in various salt solutions) was measured with a coaxial cylinder viscometer (12). The dielectric constant of aqueous solutions of dextrans was measured by the alternating current bridge method (13).

Quantification of RBC Aggregation

Microscopic Aggregation Index (MAI). Suspensions containing 1.0% RBC in various media were observed microscopically in a 100-μm deep hemocytometer. Photomicrography was taken from at least three different fields. The number of cell units in each field was counted according to the definition that one "unit" was either one monodispersed cell or one aggregate. The average number of RBC in each unit found in the dextran suspensions was calculated as the MAI:

$$MAI = N_D/\tilde{N}_S \tag{2}$$

where N_D is the number of cell units in dextran suspensions and N_S the number of cells (all monodispersed) in the dextran-free saline suspension.

Reflectometric Aggregation Index (RAI). The light reflectance of suspensions containing 45% RBC in various media was measured in a reflectometer (14) in which the suspensions can be subjected to controlled rates of shear. The light reflectance at a shear rate of 200 sec^{-1} (R_{200}), which generally caused complete disaggregation of RBC, was used as a reference point to calculate the RAI at various low shear rates or zero shear:

$$RAI_i = 1 - (R_i/R_{200}) \quad (3)$$

where R_i is the light reflectance at a shear rate of i sec^{-1} (including i = 0).

Electron Microscopy

RBC (cell concentration = 1%) were allowed to sediment in dextran solutions in a shallow polyethylene cap. After careful removal of the supernatant solution, chrome-osmium tetroxide was slowly added to the sediment. Two hours later, the sample was dehydrated with serial changes in ethanol and with propylene oxide. After embedding in an accelerated embedding monomer (Fluka AG Chemische Fabrik, Buchs SG, Switzerland), the specimen was incubated at 60°C for at least 48 hours. Thin sections were examined with an RCA Model EMU-3C electron microscope calibrated with replicas of diffraction (Ernest F. Fullam, Inc., Schenectady, N.Y.). The details of the electron microscopic technique for the measurement of intercellular distance have been published elsewhere (6).

RESULTS

Effects of Dextrans on Normal RBC in 150 mM NaCl Solution

Normal RBC were monodispersed in 150 mM NaCl solution and in the same solution containing Dx 20 up to a concentration of 10 mM/L, or 20 g% (Fig. 1). RBC aggregation was observed when larger molecular-weight dextrans were used. For each dextran, the

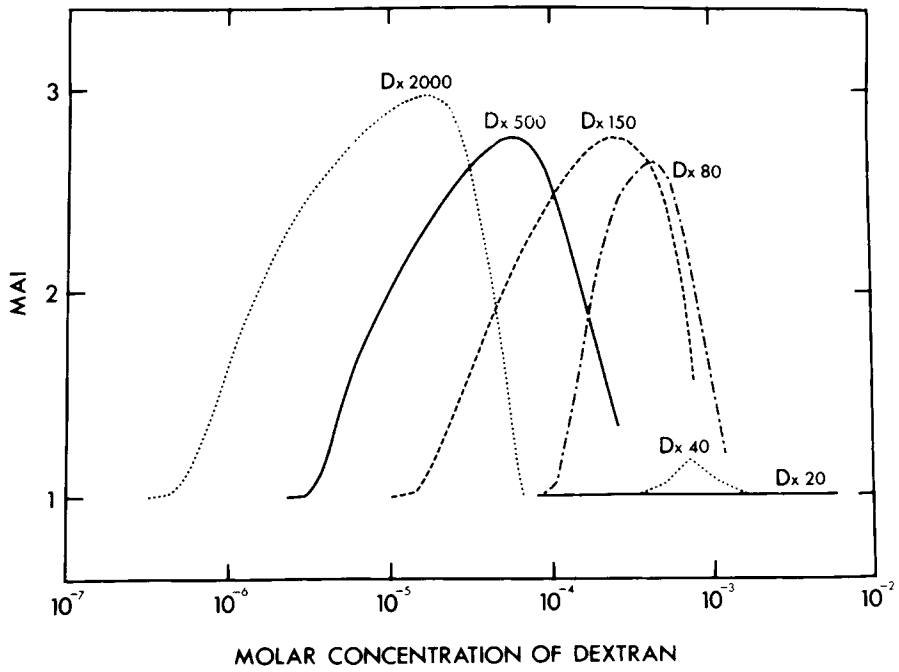

Fig. 1. Variations of the microscopic aggregation index (MAI) with the molar concentration of dextrans with various molecular weights.

degree of aggregation showed a bell-shape relation to the dextran concentration, i.e., RBC aggregation occurred only within a certain range of molar concentrations characteristic of each dextran fraction. The minimum concentration of dextran required to give detectable RBC aggregation (referred to as the critical concentration in Fig. 2) is inversely related to the molecular weight of the dextran. The relationships between critical concentration and molecular weight for the plasma proteins (albumin and fibrinogen) and the positively charged polymer (polylysines, data from ref. 15) are shown for comparison.

Electron microscopic pictures of the RBC rouleaux formed in plasma, fibrinogen solution, or dextran solutions, showed the existence of an intercellular space with a rather constant interfacial distance (Figs. 3 and 4). The relative uniformity of the intercellular spacing was associated with a deformation of the cells which usually lose their biconcave discoid shape. The intercellular distance of rouleaux in dextrans varied with the molecular size of the dextran (Fig. 5). For each dextran fraction, the intercellular distance does not vary significantly with dextran concentration.

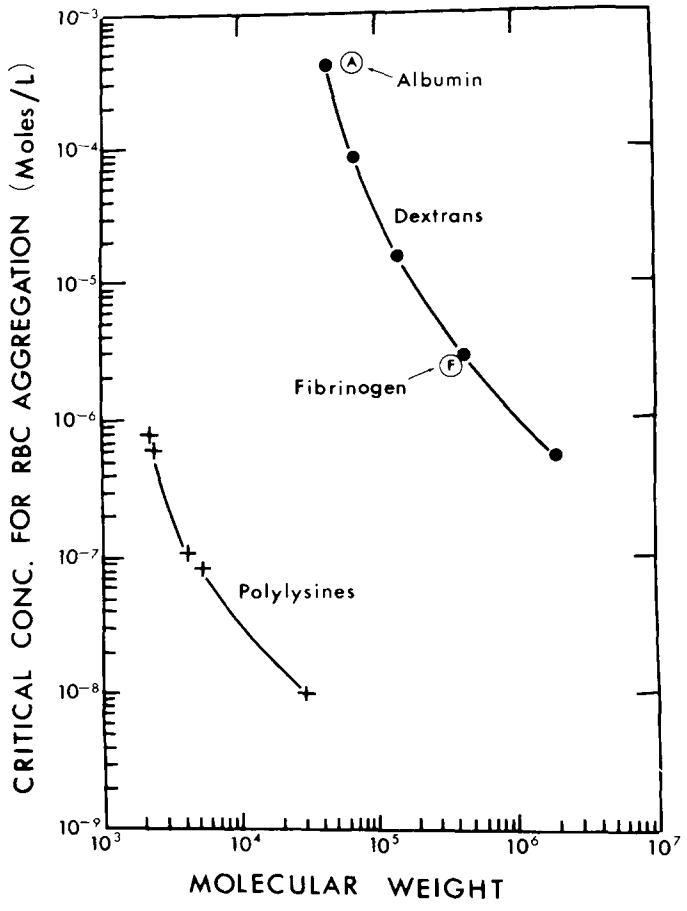

Fig. 2. The critical (or minimal) concentration of macromolecules required to induce RBC aggregation as a function of molecular weight. Note the difference in results on polylysines (15) and the data on dextrans and plasma proteins. [From (9).]

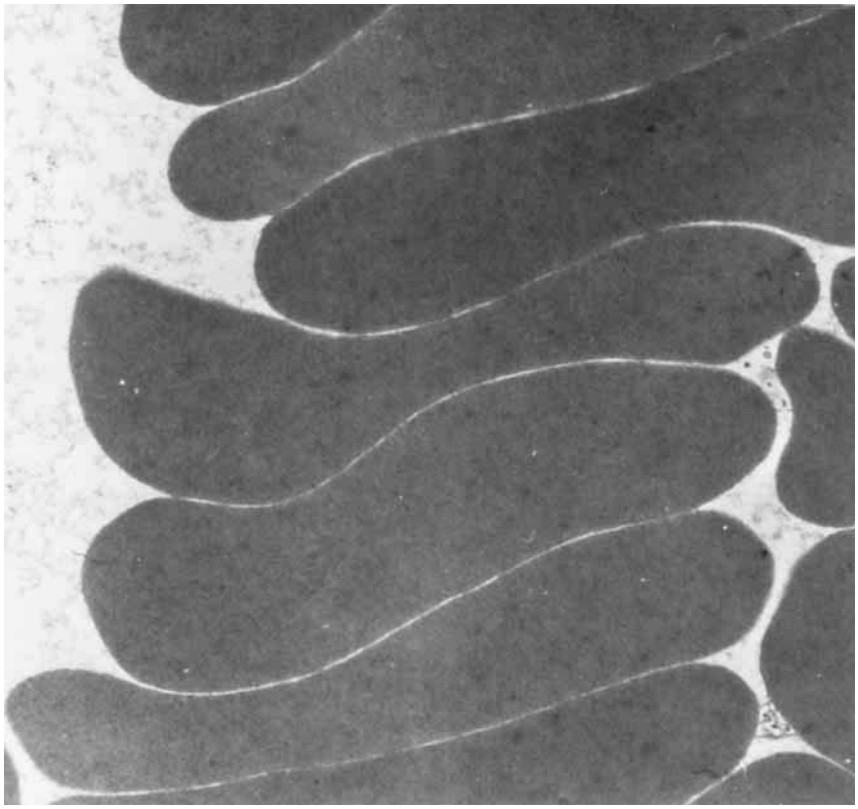

Fig. 3. Transmission electron micrographs of rouleaux of RBC in plasma. Note the parallel cell surfaces and relatively uniform intercellular distance. [From (6).]

Normal RBC in 150 mM NaCl solution had an electrophoretic mobility of -1.12 ± 0.08 (S.D.) $\mu m\ sec^{-1}/volt\ cm^{-1}$, which corresponded to a zeta potential of -15 mV. The addition of dextrans caused a reduction of RBC mobility. The results on Dx 80 are shown in Fig. 6. Dielectric constant measurements on aqueous solutions of dextrans with wide ranges of molecular sizes (Dx 20 to Dx 500) and concentrations (up to 10 g%) showed the same value as water, i.e., 78.5 at 25°C. The instrumentation used was not suitable for dielectric measurement in salt solutions, but it appears reasonable to assume that dextrans also would not change the dielectric constant of the saline solution. The viscosity of the water or saline solution, however, increased following the addition of dextran, as illustrated in Fig. 6 for Dx 80. Substitution of the results on viscosity, electrophoretic mobility, and dielectric constant into eq. 1 allowed the calculation of the zeta potential, which increases nearly linearly with an increase in dextran concentration (Fig. 6). The ratio of the zeta potential of RBC in dextran (ζ or ζ_β) to that in dextran-free saline solution (ζ_o) was calculated as

$$Z = \zeta_\beta/\zeta_o \qquad (4)$$

The increases in ζ and Z were also observed with other dextran fractions, and the effect varied directly with the molecular weight of the dextran used.

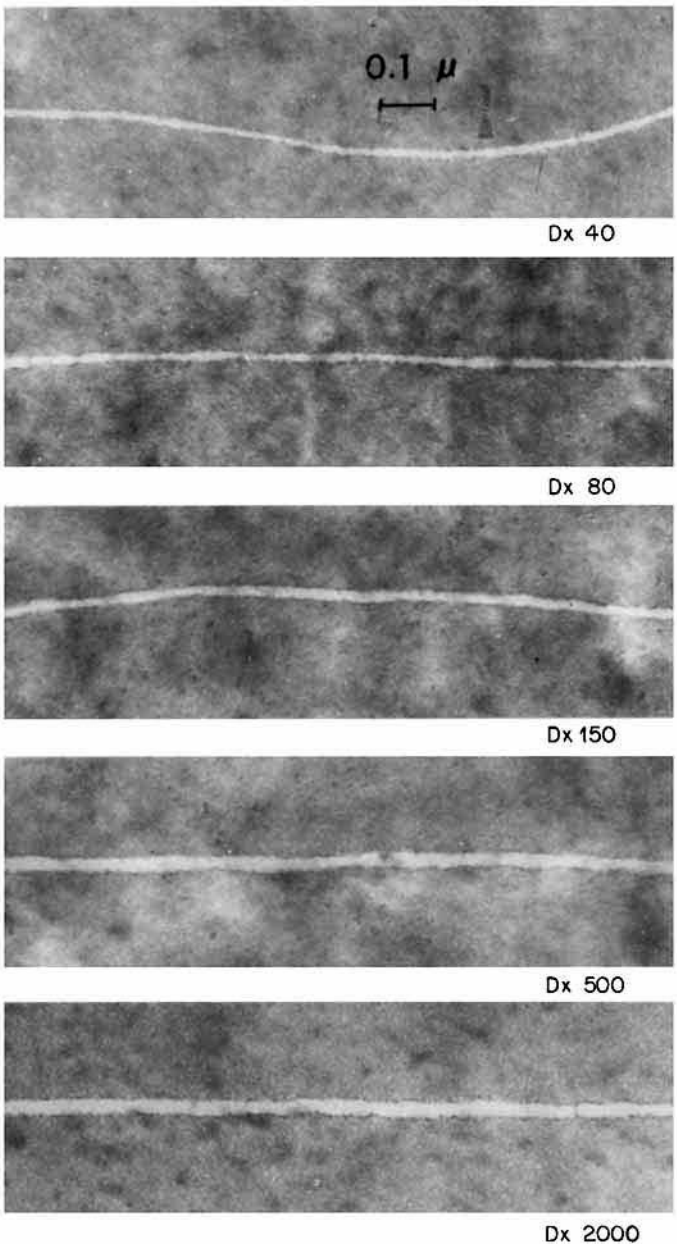

Fig. 4. Transmission electron micrographs of rouleaux of RBC in dextrans with various molecular sizes. Note the widening of the intercellular space with an increase in dextran molecular size. [From (6).]

Effects of Dextrans on Neuraminidase-Treated RBC in 150 mM NaCl Solution

Neuraminidase treatment of RBC resulted in a reduction of electrophoretic mobility (Fig. 7). Near-maximum reduction in mobility to -0.1 μm sec^{-1}/volt cm^{-1} was accomplished by the use of 15 μg of neuraminidase per ml of 1% RBC suspension in 150 mM NaCl solution, incubated at 37°C for 60 minutes. Such neuraminidase-treated

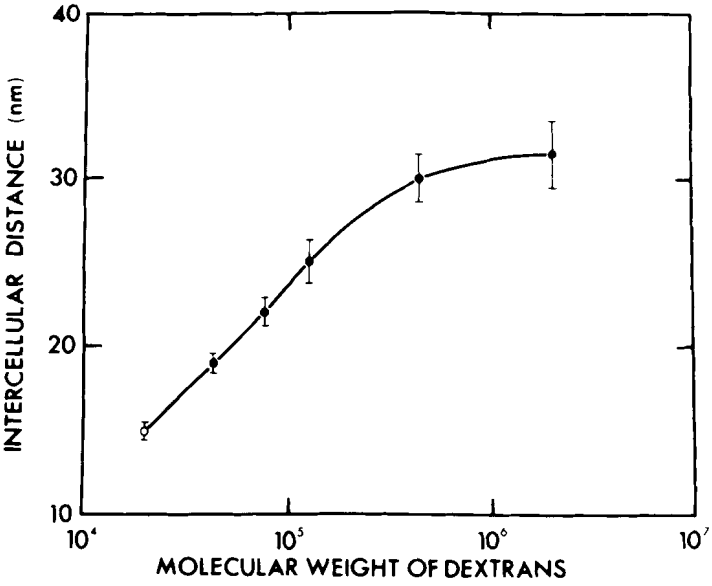

Fig. 5. Variation of the intercellular distance with the molecular weight of dextrans. The data on Dx 20 (open circle) were obtained for neuraminidase-treated RBC, and the results on larger dextrans were the same for normal and neuraminidase-treated RBC. Vertical bars denote S.E.M.

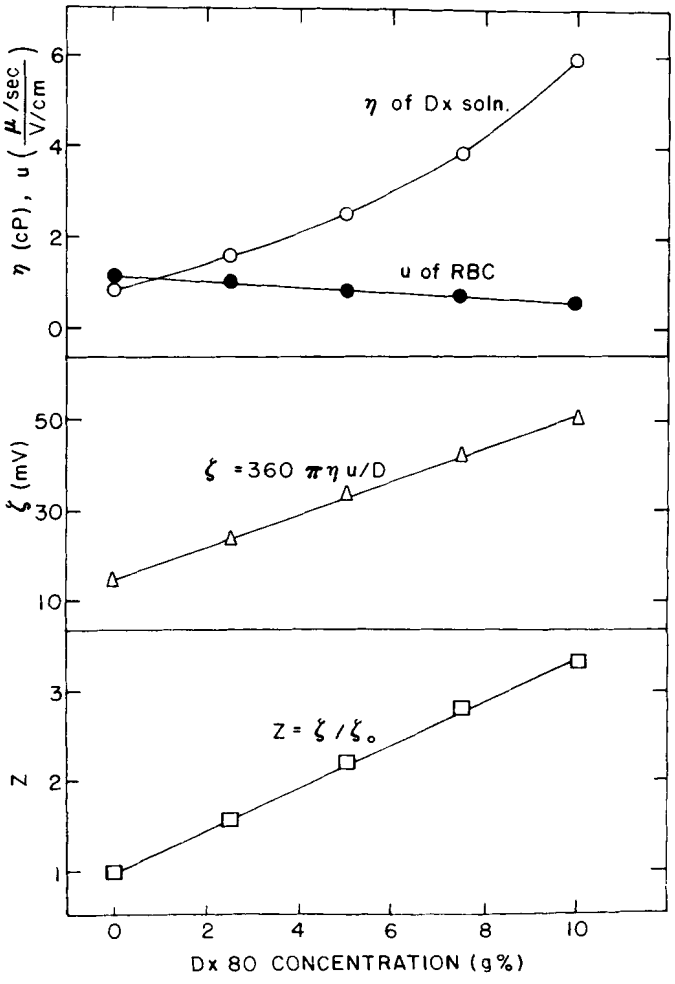

Fig. 6. Effects of Dx 80 concentration (dissolved in 150 mM NaCl solution) on electrophoretic mobility (u) of normal RBC, the viscosity (η) of the dextran solution, the zeta potential (ζ) of the RBC, and the zeta potential ratio (Z). The value for dielectric constant (D) was 78.5 for all dextran concentrations.

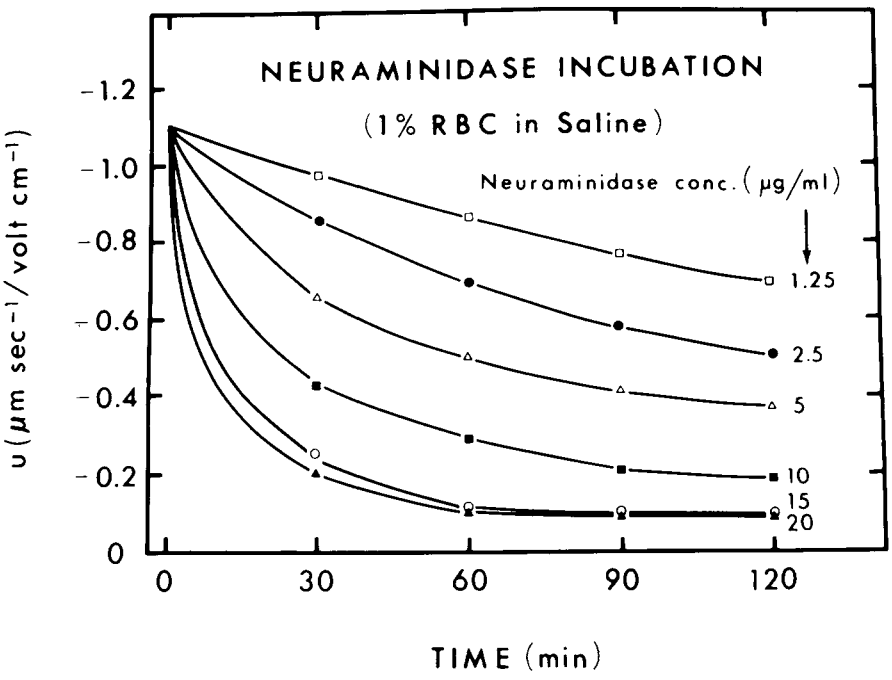

Fig. 7. Effects of neuraminidase treatment on the electrophoretic mobility of RBC. [From (7).]

(N–treated) RBC had a zeta potential of approximately −1.3 mV. The addition of dextrans caused a further reduction in the electrophoretic mobility of the N–treated RBC. The extremely slow mobility values made the calculation of zeta potential (eq. 1) relatively inaccurate, but it appears the the decrease in mobility was parallel to the increase in viscosity and that the zeta potential of N–treated RBC did not increase markedly with the addition of dextrans.

The N–treated RBC, as the normal RBC, were monodispersed in 150 mM NaCl solution. Dx 20, which did not cause any aggregation of normal RBC at all concentrations, induced significant aggregation of the N–treated RBC when the concentration of Dx 20 was above 3 g% (Fig. 8A). Dx 40, which led to only a minimum aggregation of normal RBC, caused strong aggregation of N–treated RBC (Fig. 8B). With Dx 80 up to a concentration of 4 g%, N–treated RBC exhibited only a slightly stronger aggregation than the normal RBC; but the former did not show the disaggregation phase with Dx 80 concentrations above 4 g% (Fig. 8C). There was also no disaggregation phase for N–treated RBC in high concentrations of Dx 20 and Dx 40 (Fig. 8A and B).

Electron microscopic examination of RBC rouleaux formed by the N–treated RBC showed parallel cell surfaces similar to the picture for the normal RBC. The intercellular distances for N–treated RBC in Dx 40 and larger dextrans were the same as for normal RBC in the same dextrans. Dx 20, which did not cause the aggregation of normal RBC, resulted in an intercellular distance of 15nm in the rouleaux of N–treated RBC (fig. 5).

Influence of Divalent Cations on RBC Aggregation

When 2.5–10 mM of the Na^+ in the 150 mM NaCl solution were replaced by an

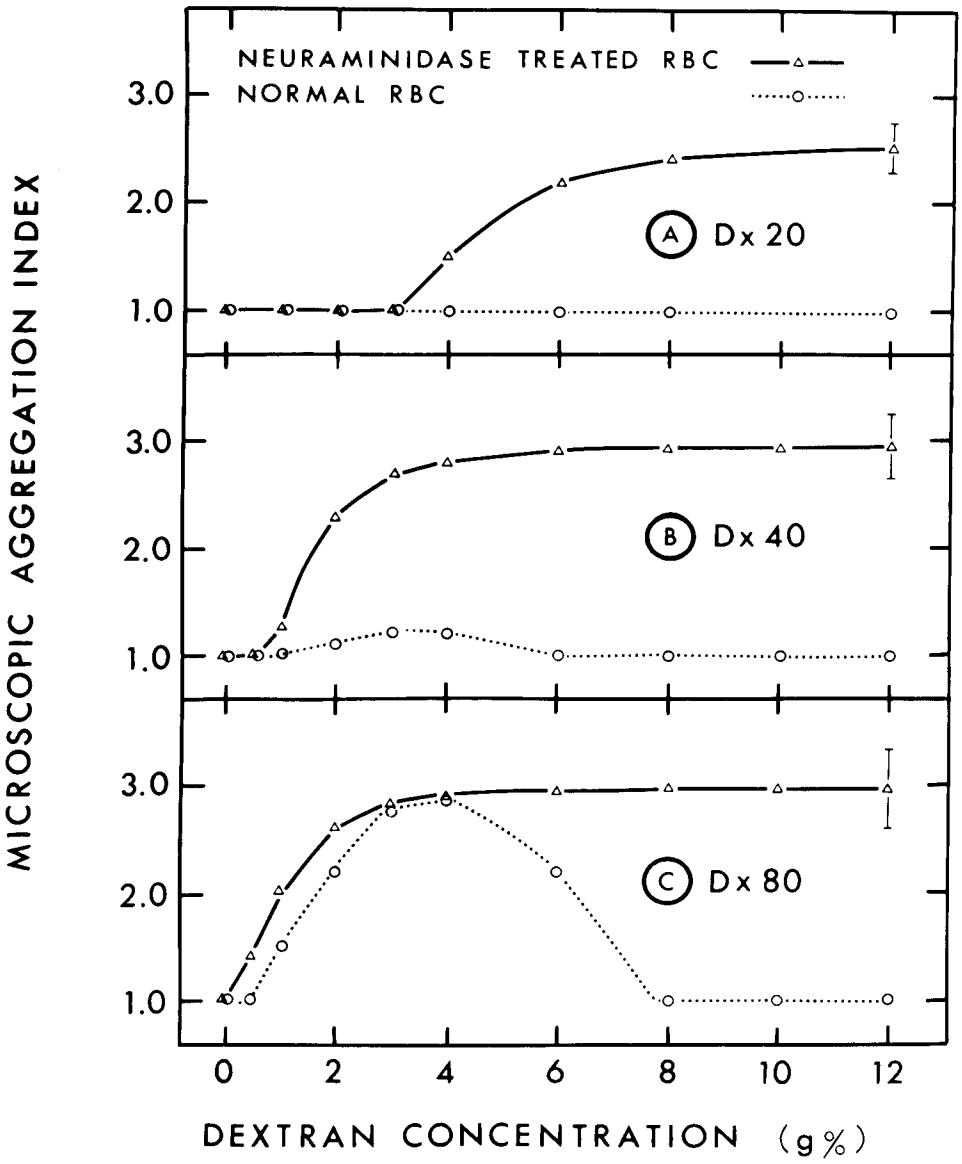

Fig. 8. Effects of Dx 20 (A), Dx 40 (B), and Dx 80 (C) on the microscopic aggregation index (MAI) of normal RBC (dotted lines) and neuraminidase-treated RBC (solid lines). Vertical bars represent S.E.M. [From (7).]

equimolar amount of Mg^{2+}, Ca^{2+}, or Ba^{2+}, the magnitudes of the electrophoretic mobility and the zeta potential of normal RBC decreased and there was no significant difference in the effects caused by the three divalent cations used (Fig. 9). The effect was even more pronounced when the trivalent cation La^{3+} was used, whereas replacement of Na^{+} by another monovalent cation K^{+} had no significant effect. Variations of the valency of the anions (e.g., comparison of $MgSO_4$ and $MgCl_2$) had no effect on the electrokinetic properties of RBC.

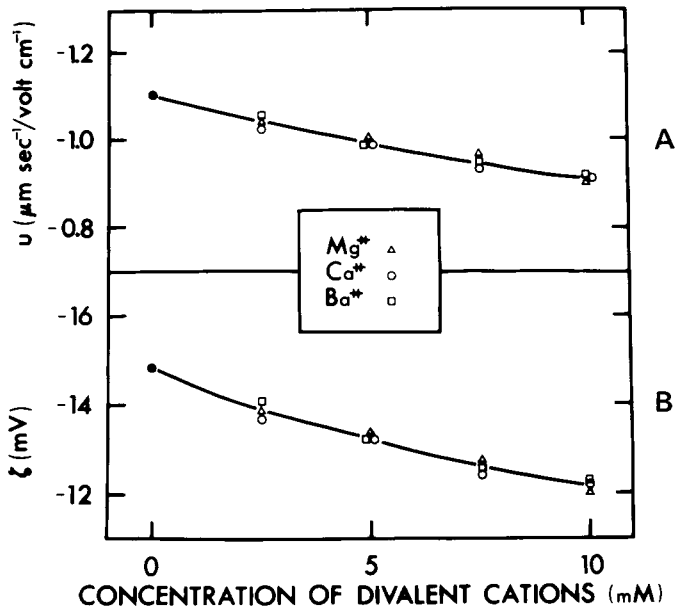

Fig. 9. Effects of divalent cations on electrophoretic mobility (A) and zeta potential (B) of normal RBC.

Replacement of Na^+ with the divalent cations resulted in an enhancement of the aggregation of normal RBC in Dx 40 and Dx 80: There was a slight increase in the degree of aggregation with dextran concentrations up to 4 g% and a suppression of RBC disaggregation at higher dextran concentrations (Fig. 10). On an equimolar basis, there was no detectable difference among the effects of Ca^{2+}, Mg^{2+}, and Ba^{2+} over the concentration range studied.

With the use of N–treated RBC, replacement of Na^+ with the divalent cations had no effect on the aggregation induced by Dx 40 or Dx 80 (Fig. 11).

Influence of Ionic Strength on RBC Aggregation

When the ionic strength of the suspending medium was reduced by an equiosmolar replacement of NaCl with sucrose, the electrophoretic mobility of normal RBC increased (Fig. 12A). With the use of a dielectric increment of –11 per mol NaCl and the data on RBC mobility and medium viscosity, the zeta potential was calculated (eq. 1) and found to increase with a reduction in ionic strength (Fig.12B).

A reduction of the ionic strength (I) of the suspending medium resulted in a decrease of the effectiveness of Dx 80 in causing the aggregation of normal RBC (Fig. 13A). In comparison to the data obtained with I = 150 mM, Dx 80 at I = 100 mM caused significantly less RBC aggregation, and the optimum Dx 80 concentration was shifted to a lower value. With a further reduction in ionic strength to I = 50 mM, Dx 80 failed to cause any aggregation of normal RBC. In contrast, the aggregation of N–treated RBC by Dx 80 was not affected by variations in the ionic strength of the solution (Fig. 13B).

Fig. 13A shows the effect of ionic strength on RBC aggregation as measured by the microscopic counting of aggregate size in suspensions containing only 1% RBC. With the

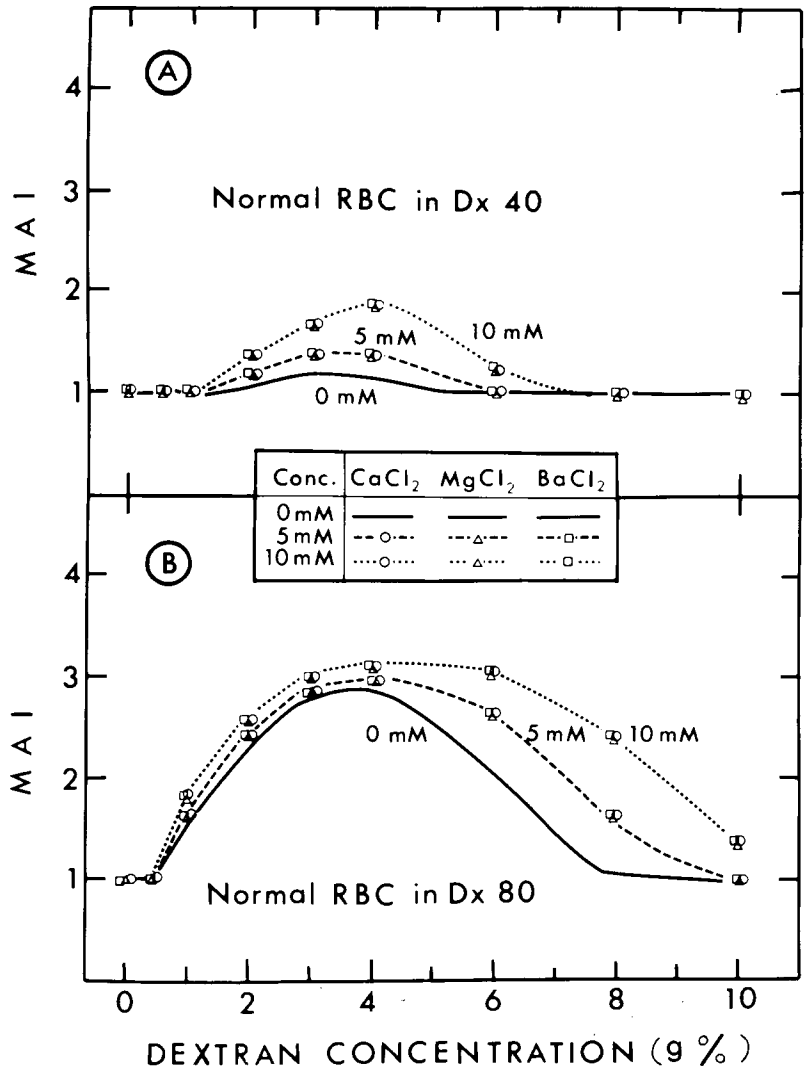

Fig. 10. Effects of divalent cations on the microscopic aggregation index (MAI) of normal RBC in Dx 40 (A) and Dx 80 (B). [From (8).]

use of the reflectometric technique, it was possible to measure RBC aggregation at a hematocrit of 45% (Fig. 14). The rise in cell concentration caused an increase in the probability of cell-to-cell encounter and hence an enhancement of RBC aggregation as compared to MAI measurements (Fig. 13A). Thus, the RAI data (at zero shear stress) indicate that there was some degree of aggregation of normal RBC by Dx 80 (1–2 g%) even when the ionic strength was reduced to 50 mM (Fig. 14).

With the use of the reflectometric technique, it also became possible to study the disaggregation of RBC by shear stress. In a suspension of normal RBC (45% hematocrit) in 2 g% Dx 80 at I = 150 mM, the degree of aggregation as measured by RAI decreased progressively with the application of shear stress (τ), and the suspension became essentially

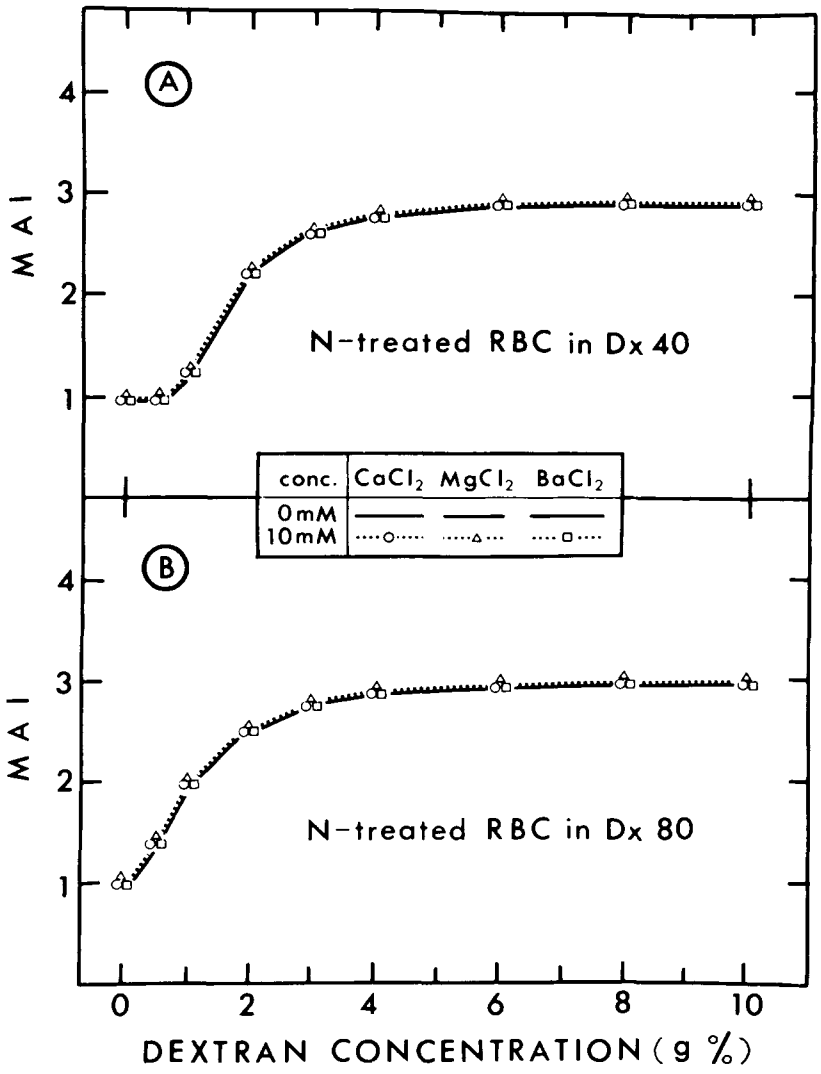

Fig. 11. Effects of divalent cations on the microscopic aggregation index (MAI) of neuraminidase-treated RBC in Dx 40 (A) and Dx 80 (B). [From (8).]

monodispersed at $\tau = 3$ dyn/cm^2 (open circles in Fig. 15A). These results of RBC disaggregation by increasing shear stress (at a constant I = 150 mM) can be compared with the data of RBC disaggregation by decreasing ionic strength (at zero shear stress, dots in Fig. 15A). Thus, in order to cause a decrease in RAI to 0.2, one can either reduce the ionic strength to 50 mM or apply a shear stress of 0.9 dyn/cm^2. In this manner, an equivalence between τ and I can be established (Fig. 15B).

DISCUSSION

In a suspending medium free of macromolecules, normal as well as N–treated RBC

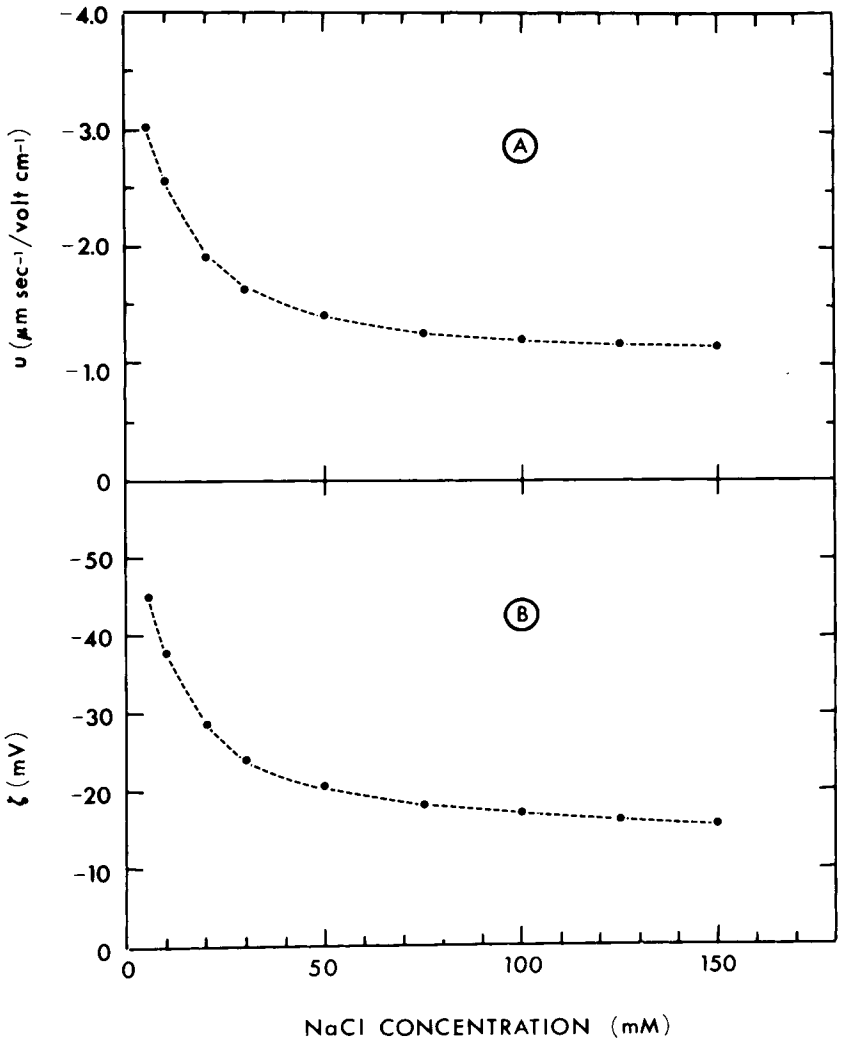

Fig. 12. Effects of ionic strength on electrophoretic mobility (A) and zeta potential (B) of normal RBC in mixtures of NaCl and sucrose with the total osmolality maintained at 300 mOsm.

exist as monodispersed cells (Fig. 8). Therefore, the aggregation of RBC does not result from any adhesive force existing directly between RBC surfaces, but rather depends on the interaction between the cell surface and the macromolecules in the suspending medium.

As a result of the finding that the aggregating effectiveness of the macromolecule and the intercellular distance in RBC rouleaux both vary directly with the size of the macromolecule used to induce aggregation, we have proposed a model of RBC aggregation by macromolecular bridging (5, Fig. 16). In this model, it is postulated that the terminal portions of each bridging macromolecule are adsorbed to the two adjacent cell surfaces in the rouleaux, leaving a central bridge in the intercellular space. The adsorption of dextran molecules to RBC surface has been demonstrated recently by Brooks (16) with the use of C^{14}- labeled Dx 80. As shown in Fig. 17, the adsorption isotherm of Dx 80 is

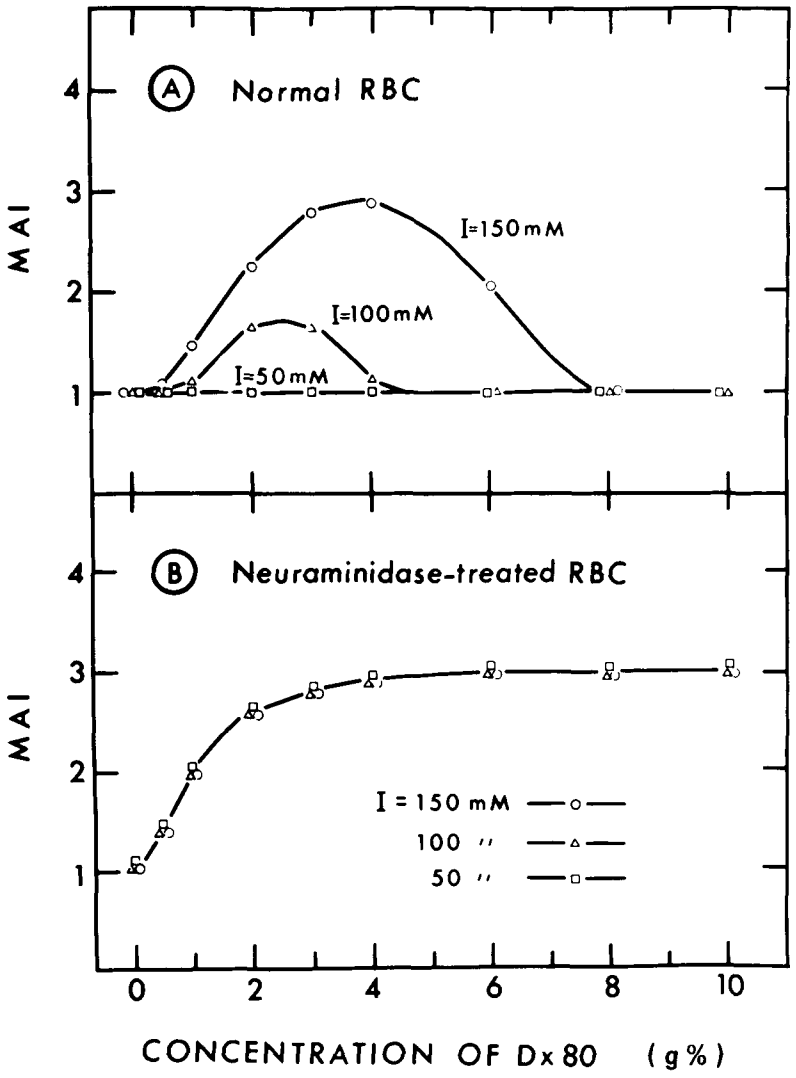

Fig. 13. Effects of ionic strength (I) on the microscopic aggregation index (MAI) of normal (A) and neuraminidase-treated RBC (B) in Dx 80. The total osmolality of the NaCl-sucrose mixture was maintained at 300 mOsm. [From (8).]

essentially linear over a wide range of dextran concentrations.

The negative surface charge of the normal RBC leads to a surface potential which is approximated by the zeta potential obtained from electrophoretic mobility measurements (17). The surface potentials of adjacent RBC in the rouleuax result in an electrostatic repulsive force which is inversely related to the distance of separation. The removal of the sialic acid from the cell surface by neuraminidase treatment caused marked reductions of the surface charge and surface potential (Fig. 7). Such charge-depleted RBC were aggregated by Dx 20 with an intercellular distance of 15 nm (Fig. 5). In the presence of the normal RBC surface charge, the electrostatic repulsive force apparently was too

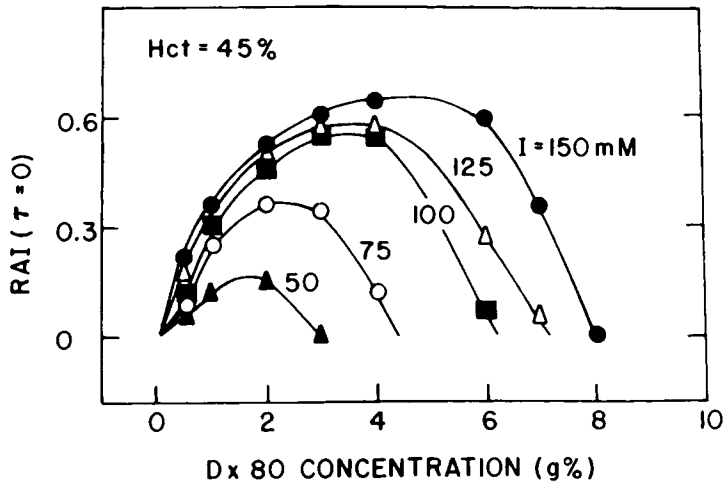

Fig. 14. Effects of ionic strength (I) on the reflectometric aggregation index (RAI) of normal RBC in Dx 80 at zero shear stress ($\tau = 0$). The total osmolality of the NaCl-sucrose mixture was maintained at 300 mOsm.

large over this relatively short intercellular distance for cell aggregation to occur (Fig. 8A). A comparison of the aggregation of normal and N–treated RBC in response to Dx 40 (Fig. 8B), Dx 80 (Fig. 8C), and larger dextrans (not shown in Fig. 8) provides further evidence that the electrostatic repulsive force becomes less important when the intercellular distance is widened.

The relation between surface charge, surface potential, and electrostatic repulsive force is affected by the ionic environment at the cell surface (3). The presence of counterions (cations in this case) in the suspending medium causes a screening of the surface charge and leads to a decrease in surface potential at a given surface charge density. The existence of surface charge groups causes the formation of an electric double layer in which the potential decreases with the distance from cell surface. The degree of screening of surface charge and the slope of the potential decrease (or the reciprocal of the double layer thickness) in the electric double layer are determined by the concentration and valency of the counterions in the suspending medium. A replacement of the monovalent cation Na^+ by the divalent cations should cause a decrease of surface potential and a shrinkage of the double layer, leading to a reduction in electrostatic repulsive force. The present experimental studies indeed show that divalent cations cause a decrease in zeta potential (Fig. 9B) and an increase in aggregation of the normal RBC (Fig. 10), but not the N–treated RBC (Fig. 11). Conversely, a reduction of the ionic strength (a decrease in cation concentration) should lead to an increase of surface potential, an expansion of the double layer, and an enhancement of electrostatic repulsive force. This prediction is again verified by the experimental findings that decreases in ionic strength cause an increase in zeta potential (Fig. 12B) and a decrease in aggregation of the normal RBC (Fig. 13A), but not the N–treated RBC (Fig. 13B).

In the preceding paragraphs, the influences of intercellular distance (d), sur-

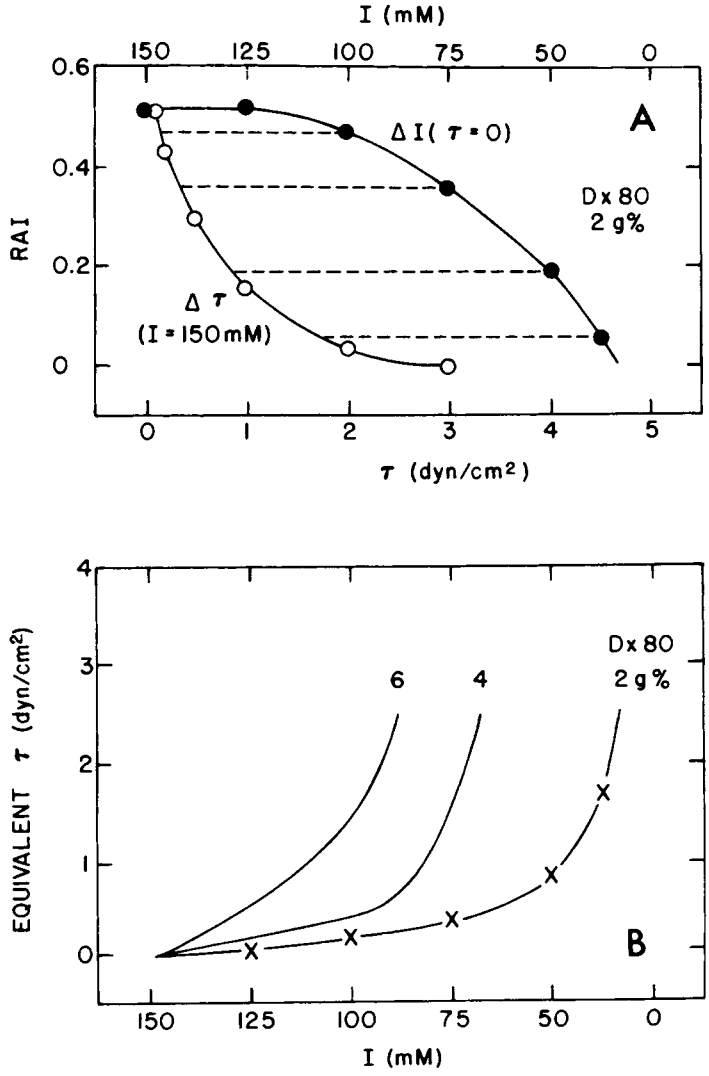

Fig. 15. Decreases of the reflectometric aggregation index (RAI) of normal RBC in 2 g% Dx 80 by reduction in ionic strength (ΔI, solid dots, upper abscissa) and by increase in shear stress ($\triangle\tau$, open circles, lower abscissa). The horizontal lines give the values for ionic strength (I) and shear stress (τ) that cause equivalent degrees of RBC disaggregation, which are cross plotted in B (crosses). Also shown in B are the equivalent values of τ and I which gave the same RAI for RBC in 4 and 6 g% Dx 80.

face potential (estimated by ζ), cation valency (z), and ionic strength (I) on the electrostatic repulsive force (F_e) between adjacent red cell surfaces in the rouleaux have been discussed. These relations can be expressed quantitatively by the use of equations derived in colloid chemistry (3). Since electron microscopic study has shown that adjacent RBC surfaces in the rouleaux are parallel to each other (Fig. 4), the geometry of the system is essentially that of parallel plates with uniform separation. Hence, the electrostatic repulsive pressure (P_e), which is the electrostatic repulsive force per unit surface area, can be expressed as

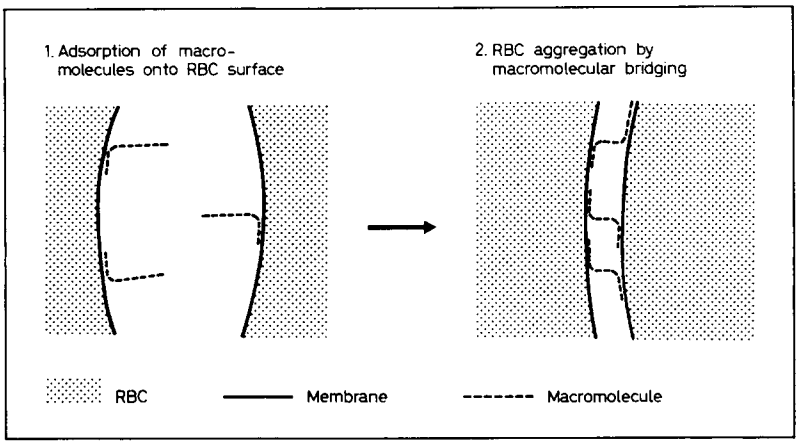

Fig. 16. A model of RBC aggregation by macromolecular bridging. [From (5).]

$$P_e = 0.064\ IRT \tanh^2(z\epsilon\zeta/4kT)e^{-\kappa d}$$

where I is the ionic strength in moles per liter, R is the gas constant, T is the absolute temperature, ϵ is the electronic charge, k is the Boltzmann constant, and κ is the slope of the potential drop in the double layer.*

$$\kappa = \sqrt{8\pi\epsilon^2 NIz^2/1000DkT} \tag{6}$$

where N is Avogadro's number. Equations 5 and 6 indicate that P_e varies directly with ζ or z and inversely with I or d. For normal RBC (ζ = 15 mV) suspended in 150 mM NaCl solution (z = 1), eq. 5 becomes

$$P_e = 5 \times 10^6\ e^{-1.29d} \tag{7}$$

where P_e is in dyn/cm^2 and d is in nm.

In the presence of macromolecules, such as dextrans, which occupy a significant volume in the suspension, the effective ionic strength per unit volume of the suspending medium decreases because of volume exclusion by the macromolecule (4). This effect would be most pronounced at the cell surface, where macromolecular adsorption leads to a local increase in macromolecule concentration. As a result, the addition of dextrans to a suspension of normal RBC would lead to an increase in zeta potential from ζ_0 to ζ_β (Fig. 6) and a widening of the double layer (i.e., a decrease in the slope of the potential drop from κ_0 to κ_β); these changes occur without any alteration in the cell surface charge. Theoretical treatment by Brooks (4) has shown that

$$\frac{\zeta_\beta}{\zeta_0} = \frac{\kappa_0}{\kappa_\beta} \tag{8}$$

if the location of the shear plane is unaffected by the adsorbed macromolecule and if the ionic strength is not excessively reduced (i.e., the product of the thickness of the adsorbed layer and κ_β is maintained above 2). Since κ is proportional to the square root of the ionic strength (eq. 6), it follows that

*In the equation employed previously by the authors (7, 8) to calculate the electrostatic repulsive pressure, the constant 64 was used instead of the value 0.064 in equation 5. Therefore, the results reported in these papers (7, 8) were too high, and should be multiplied by 10^{-3}.

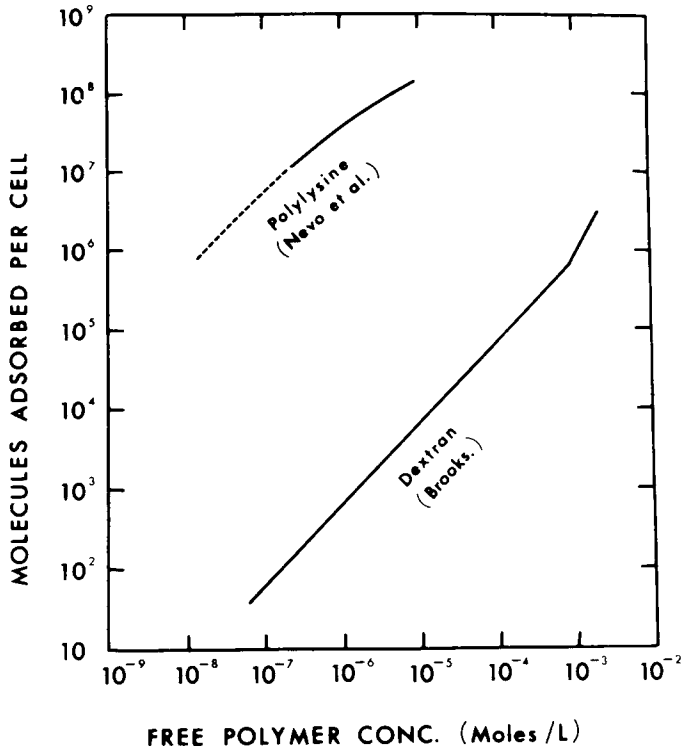

Fig. 17. Adsorption isotherms for Dx 80 [from (16)] and polylysine [polymer containing 36 lysine molecules, from (18)] on normal RBC.

$$Z = \frac{\zeta_\beta}{\zeta_0} = \frac{\kappa_0}{\kappa_\beta} = \frac{\sqrt{I_0}}{\sqrt{I_\beta}} \tag{9}$$

Where I_0 and I_β refer, respectively, to the nominal ionic strength of the solution (before the addition of dextran) and the effective ionic strength of the solution containing dextran. Therefore, if ζ and ζ_0 are determined, I_0 is known and κ_0 calculated from eq. 6, then I_β and κ_β can also be calculated with the use of eq. 9. Use of I_β, ζ_β, and κ_β in eq. 5 yields an expression for the electrostatic repulsive pressure in the presence of dextran.

$$P_e = 0.064\, I_\beta RT \tanh^2 (z\epsilon\zeta_\beta/4kT) e^{-\kappa_\beta d} \tag{10}$$

With the use of the values of Z obtained at various dextran concentrations (Fig. 6), the corresponding values of P_e can be caluclated from eq. 10. Figure 18 shows the exponential relations between P_e and the distance of separation for several concentrations of Dx 80 in 150 mM NaCl: The curves are shifted upward as Dx 80 concentration is increased. Since electron microscopic studies have shown an intercellular distance of 22 nm for RBC in Dx 80, the P_e values at d = 22 nm represent the electrostatic repulsive pressures opposing RBC aggregation by various concentrations of dextran.

Figure 19 shows that this electrostatic repulsive pressure (d = 22 nm in Fig. 18) increases with an increase in Dx 80 concentration. A decrease in the NaCl concentration

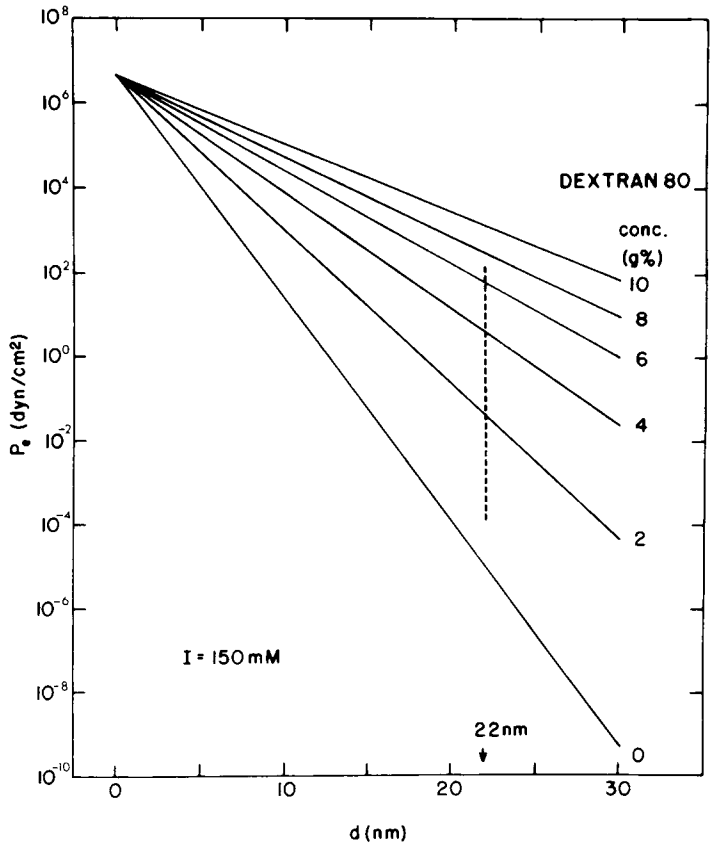

Fig. 18. Electrostatic repulsive pressure between normal RBC surfaces (P_e, eq. 10) as a function of the distance of separation (d). Note the rises in P_e curves with increases in Dx 80 concentration (dissolved in 150 mM NaCl). The vertical dotted line indicates d = 22 nm, which is the intercellular distance for RBC in Dx 80.

from 150 mM to 100 and 50 mM causes the curve to shift to the left, indicating that a decrease in I_0 has a similar effect on P_e as the decrease in I_β due to volume exclusion by dextran. In the absence of mechanical shearing force, the net aggregating force per unit area of cell surface (P_a) represents a balance between the macromolecular bridging force per unit area and the electrostatic repulsive pressure:

$$P_a = P_b - P_e \tag{11}$$

The reflectometric aggregation index obtained at a high cell concentration of 45% and at zero shear stress (Fig. 14) reflects the net P_a in the RBC–dextran system. With the P_e vs. Dx 80 concentration curve shown in Fig. 19A (solid line marked I = 150 mM), a P_b vs. Dx 80 concentration curve (dotted line in Fig. 19A) with an exponential growth toward a saturation level would give a net P_a (Fig. 19B) which shows the same variation with Dx 80 concentration as the experimentally determined RAI (Fig. 19C). When differences between this P_b curve (dotted line in Fig. 19A) and the P_e curves for I = 100 and 50 mM (solid lines in Fig. 19A) are plotted against the Dx 80 concentration (Fig. 19B), these net P_a curves again show general agreement with the RAI data obtained for the respective ionic strengths (Fig. 19C). An even better agreement would be obtained if P_b curves with

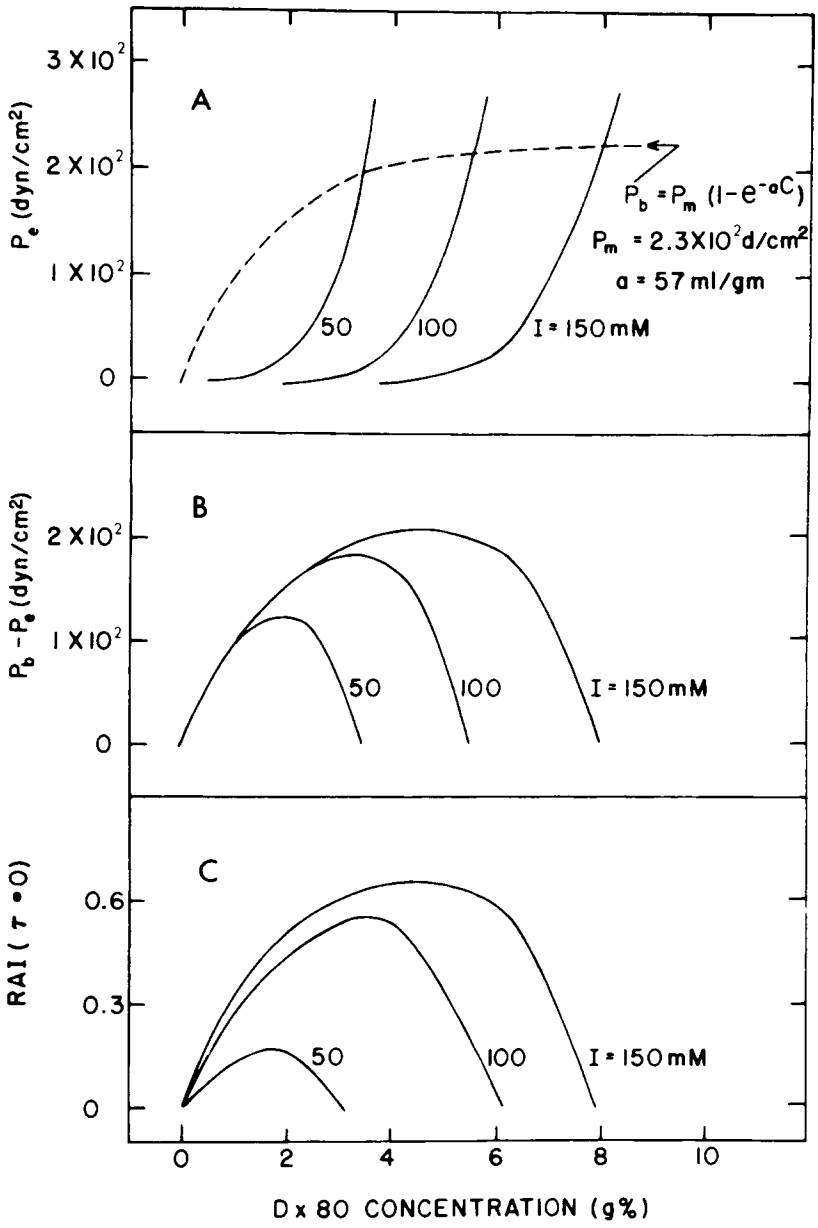

Fig. 19. Solid lines in A represent the relation between electrostatic repulsive pressure (P_e) and the Dx 80 concentration, at three ionic strengths (I = 150, 100, and 50 mM). The dotted line in A represents the theoretical bridging pressure (P_b) as a function of Dx 80 concentration. The P_b curve is chosen such that the relation between $P_b - P_e$ and Dx 80 concentration (B) is similar to that found between reflectometric aggregation index and Dx concentration (C).

smaller values of a (see equation in Fig. 19A) are used for these low ionic strengths. In the N–treated RBC, P_e should be negligible and P_a equals P_b in the absence of shear stress (Fig. 11). The relation between the aggregation of N–treated RBC and Dx 80 concentration (Fig. 8C), which reflects the net P_a for aggregation, indeed has the same form as the P_b curve obtained in Fig. 19A (dotted line).

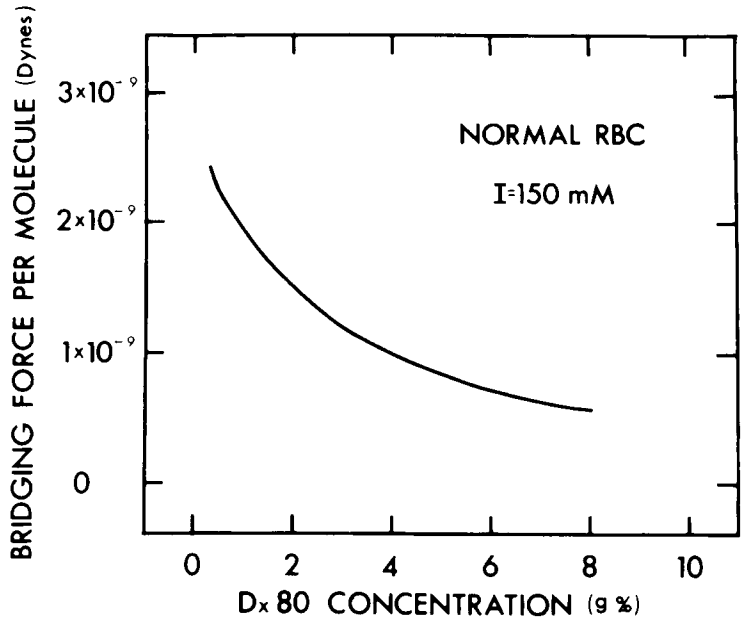

Fig. 20. Relation between the bridging force per adsorbed Dx 80 molecule and the Dx 80 concentration.

A combination of the macromolecular bridging force per unit area (P_b) deduced in Fig. 19 and the adsorption isotherm determined by Brooks (16) for Dx 80 on normal RBC (Fig. 17) allows a calculation of the bridging force per adsorbed macromolecule (f_b). The results of such calculation show that the bridging force per adsorbed molecule decreases with an increase in dextran concentration (Fig. 20). This may be explained by a decrease in the number of adsorption bonds (or segments) per molecule as the number of dextran molecules adsorbed per unit surface area increases.

The adsorption of the neutral macromolecule dextran and the negatively charged proteins (e.g., fibrinogen) onto the RBC surface probably results from relatively weak and nonspecific adsorption force, such as van der Waals force, and the adsorption does not require the presence of the negative surface charge groups. In contrast, the positively charged macromolecules, such as polylysine, are adsorbed onto the negative charge groups on the RBC surface by electrostatic attractive force, which is stronger than the van der Waals force. The difference in the nature of surface adsorption is reflected by the much lower concentration of polylysines required to achieve RBC aggregation (Fig. 2) and by the much higher affinity of the polylysine molecules for the RBC surface (18) shown by adsorption isotherm studies (Fig. 17).

The macromolecular bridging pressure (P_b) deduced from the electrostatic repulsive pressure (P_e) is in the range of 3×10^2 dyn/cm^2 (Fig. 19A). In contrast, the shear stress required to cause RBC disaggregation is in the range of 3 dyn/cm^2 (Fig. 15). Therefore, the shear stress is more effective than the electrostatic repulsive pressure by 100 fold. This discrepancy may be explained by the difference in the cell surface area over which the forces act to cause RBC disaggregation. The electrostatic repulsive force must act over the entire area of aggregation, whereas the mechanical shearing force is probably concentrated on a limited area where disaggregation occurs by a peeling process. This difference may be analogous to that existing between the force required to lift one adhesive

tape from another all at once and the force needed to separate the tapes by gradual peeling from one end to another; it is a common experience that the magnitude of the latter force is much smaller than the former.

The present study indicates that RBC aggregation is a process which represents a balance of forces at the cell surfaces. Over an area of aggregation, the net aggregating force (F_a) is equal to the macromolecular bridging force (F_b) minus the electrostatic repulsive force (F_e) and mechanical shearing force (F_s). Since the adjacent cell surfaces are deformed from the biconcave shape to the parallel plate geometry (Fig. 4), the bridging may also have to overcome the membrane bending force (F_m). Thus:

$$F_a = F_b - F_e - F_s - F_m \tag{12}$$

The macromolecular bridging force is a function of the adsorption force per macromolecular bond (f), the number of bonds adsorbed on the RBC surface per molecule (b), and the number of molecules adsorbed per unit cell surface area (n):

$$F_b = (f)\,(b)\,(n) \tag{13}$$

The number of macromolecules adsorbed per unit cell surface area is a function of the macromolecular concentration and the affinity between RBC surface and the macromolecule (Fig. 17). The number of bonds adsorbed on the RBC surface per macromolecule is a direct function of the macromolecular size and may also be inversely related to macromolecular concentration (Fig. 20). The influence of macromolecular concentration on n probably dominates over its effect on b at low macromolecular concentrations, and F_b increases with the concentration (Fig. 19A). At high macromolecular concentrations, the balance of the opposing changes in b and n probably forms the basis of the leveling of F_b. The adsorption force per macromolecular bond varies with the nature of the adsorption and is a function of the physicochemical properties of the macromolecule and the RBC surface.

The electrostatic repulsive force, as shown by eq. 5, is a function of the RBC surface potential (as measured by ζ), the slope of the potential drop in the double layer (κ) and the distance of separation between adjacent cell surfaces (d). The value of κ is a direct function of cationic strength and valency of the suspending medium. Our investigations (9) and the studies of Brooks (4) indicate that the effective ionic strength can be reduced by the presence of macromolecules due to a volume exclusion effect. This influence of macromolecular concentration on effective ionic strength is demonstrated not only with dextran but also with the plasma proteins (unpublished observations). Therefore, F_e varies inversely with the ionic strength or cationic valency and directly with the macromolecular size and concentration. Hence, an increase in macromolecular concentration has two opposing effects on RBC aggregation via its effects on F_b and F_e. With an increase in macromolecular concentration (C) up to an optimum level, the increase in F_b predominates (Fig. 19A) and there is an increase in RBC aggregation (Fig. 19B). Because of the saturation relationship between F_b and C and the exponential rise of F_e with C (Fig. 19A), the net aggregating force decreases at very high macromolecular concentrations (Fig. 19B). These alterations in the balance of forces at the cell surface may explain the biphasic changes in RBC aggregation with an increase in macromoleuclar concentration (Figs. 1 and 19C). The distance of cell separation in the rouleaux is a function of the macromolecular size (Fig. 5). Therefore, the inability of the short dextrans to aggregate RBC (Fig. 1) is attributable partially to the low F_b due to small b

(eq. 13) and partially to the large F_e as a result of the small d (eq. 5). In contrast, the longer dextrans are more effective in causing RBC aggregation (Fig. 1) because of the larger F_b due to a greater value for b and the smaller F_e resulting from the large d, unless F_e is increased by the volume exclusion effect at very high dextran concentrations.

The mechanical shearing force is a function of the shear rate and the viscosity of the suspension. However, a slight increase of shear rate (e.g., from 0 to 0.5 sec^{-1}), by increasing the probability of cell-to-cell encounter, may cause an increase in RBC aggregation. The probability of cell-to-cell encounter can also be facilitated by increasing the cell concentration, decreasing the medium viscosity, or raising the temperature. Large increases in shear rate, by increasing the shear stress, cause RBC disaggregation (Fig. 15, refs. 19–22). At a given shear rate, the disaggregating shear stress rises with the viscosity of the fluid medium, which is a function of macromolecular size and concentration. This factor may act synergistically with the electrostatic repulsive force to cause RBC disaggregation at high macromolecular concentrations.

The membrane bending force is probably small in normal RBC, because of the low bending modulus (23, 24). When there is a reduced RBC deformability, however, the increase in bending modulus may prevent the formation of parallel cell surfaces with multiple bridges and cause a reduction in RBC aggregation (25).

This type of force balance at RBC surface may have important implications in other physiological systems. The surfaces of most cells and intracellular particles (e.g., synaptic vesicles) are negatively charged (26, 27), and the surfaces are often separated by a distance of the order of 15 nm (28). The presence of macromolecules, especially proteins, in the vicinity of these surfaces reduces the effective ionic strength and increases the electrostatic repulsive force. Divalent cations, especially Ca^{2+}, play a significant role in the physiological modulation of interactions between the cell surfaces and the particulate surfaces. Although the action of Ca^{2+} is in many cases due to specific binding of this ion with the surface constituents, it may also in some cases be attributable to changes in electrostatic repulsive force between surfaces. Thus the force balance demonstrated in the present study on RBC surfaces may possibly be applied to a wide variety of surface interactions, e.g., platelet aggregation, thrombus formation (29), tumor metastasis, exocytosis of secretory granules, release of transmitter from the synaptic vesicles (27, 30), etc. For instance, the adrenergic vesicles have a similar surface charge as the RBC (27) and are released in response to Ca^{2+} influx (31). It is possible that the Ca^{2+} ion causes a fusion of the synaptic vesicle with the membrane of the nerve terminal by reducing the electrostatic repulsive force between these surfaces.

ACKNOWLEDGMENTS

The authors thank Dr. Shunichi Usami for his advice and help in the reflectometric technique. We wish to acknowledge the valuable technical assistance of Ignacio Alvarez de la Campa, Dagmara Igals, Orlando M. Leyva, and Juan Rodriguez, and the excellent secretarial help of Miss Ethel M. Goodrich.

This investigation was supported by Research Grant HL-06139 from the National Heart and Lung Institute, the U.S. Army Medical Research and Development Command Contract DADA-17-72-C-2115, and by generous gifts from The Scaife Family Charitable Trusts of Pittsburgh, Pa., and Mrs. George W. Perkins.

Dr. Kung-ming Jan is a Postdoctoral Fellow of the New York Heart Association.

REFERENCES

1. Fåhraeus, R., Physiol. Rev. 9:241–274 (1929).
2. Cook, G. M. W., Heard, D. H., and Seaman, G. V. F., Nature 191:44–47 (1961).
3. Overbeek, J. Th. G., In "Colloid Science," H. E. Kruyt, (Ed.), pp. 245–277, Elsevier, Amsterdam (1952).
4. Brooks, D. E., J. Colloid, Interface Sci. 43:687–699 (1973).
5. Chien, S., Luse, S. A., Jan, K.-M., Usami, S., Miller, L. H., and Fremount, H., Proc. 6th Eur. Conf. Microcirculation, J. Ditzel and D. H. Lewis (Eds.), pp. 29–34, Karger, Basel (1971).
6. Chien, S., and Jan, K. -M., Microvascular Res. 5:155–166 (1973).
7. Jan. K. -M., and Chien, S. J., Gen. Physiol. 61:638–654 (1973).
8. Jan, K. -M., and Chien, S. J. Gen. Physiol. 61:655–668 (1973).
9. Chien, S. Proc. 7th Eur. Conf. Microcirculation, J. Ditzel and D. H. Lewis, (Eds.), Karger, Basel Bibliotheca Anatomica 11:244–250, 303–309 (1973).
10. Ponder, E., "Hemolysis and Related Phenomena." Grune and Stratton, N.Y. (1948).
11. Bangham, A. D., Flemans, R., Heard, D. H., and Seaman, G. V. F., Nature 182:642–644 (1958).
12. Chien, S., Usami, S., Dellenback, R. J., and Bryant, C. A., Biorheology 8:35–57 (1971).
13. Pollak, W., Hager, H. J., Reckel, R., Toren, T. A., and Singher, H. O., Transfusion 5:158–183 (1965).
14. Usami, S., and Chien, S., Proc. 7th Eur. Conf. Microcirculation, J. Ditzel, and D. H. Lewis, (Eds.), Karger, Basel, (1973) (in press).
15. Katchalsky, A., Danon, D., Nevo, A., and DeVries, A., Biochim. Biophys. Acta 33:120–138 (1959).
16. Brooks, D. E., J. Colloid. Interface Sci., 43:700–713 (1973).
17. Hayden, D. A., Proc. Roy. Soc. Ser. A. 258:319–328 (1960).
18. Nevo, A., DeVries, A., and Katchalsky, A., Biochim. Biophys. Acta 17:536–547 (1955).
19. Brooks, D. E., Goodwin, J. W., and Seaman, G. V. F., J. Appl. Physiol. 28:172–177 (1970).
20. Chien, S., Usami, S., Dellenback, R. J., and Gregersen, M. I., Am. J. Physiol. 219:143–153 (1970).
21. Goldsmith, H. L., Biorheology 7:235–242 (1971).
22. Schmid-Schönbein, H., and Wells, R. E., Ergeb. Physiol. 63:146–219 (1971).
23. Fung, Y.C., Federation Proc. 25:1761–1772 (1966).
24. Skalak, R., In "Biomechanics, Its Foundations and Objectives" Y. C. Fung, N. Perrone, and M. Anliker (Eds.), pp. 457–499, Prentice-Hall, Englewood Cliffs, N.Y. (1972).
25. Chien, S., In "Hemodilution, Theoretical Basis and Clinical Application" K. Messmer and H. Schmid-Schönbein, (Eds.), pp. 1–40, Karger, Basel (1972).
26. Ambrose, E. J. (Ed.), "Cell Electrophoresis." Little, Brown, Boston (1965).
27. Neumann, E., and Rosenheck, K. J., Membrane Biol. 10:279–290 (1972).
28. Robertson, J. D., Biochem. Soc. Symp. 16:3–43 (1959).
29. Sawyer, P. N. (Ed.), "Biophysical Mechanisms in Vascular Homeostasis and Intravascular Thrombosis." Appleton, New York (1965).
30. Geffen, L. B., and Livett, B. G., Physiol. Rev. 51:98–157 (1971).
31. Douglas, W. W., Pharmacol. Rev. 18:471–480 (1966).